



## CHAPTER IV MANUSCRIPT

### **Electroactive Styrene-Isoprene-Styrene Triblock Copolymer: Effect of Morphology and Electric Field**

K. Thongsak<sup>1</sup>, A. Sirivat<sup>1,\*</sup>, and W. Lerdwijitjarud<sup>2</sup>

<sup>1</sup>*The Petroleum and Petrochemical College, Chulalongkorn University, Bangkok, 10330, Thailand.*

<sup>2</sup>*Department of Materials Science and Engineering, Faculty of Engineering and Industrial Technology, Silpakorn University, Sanamchandra Palace Campus, Nakhon Pathom 73000, Thailand.*

#### **Abstract**

Various morphological films of styrene-isoprene-styrene triblock copolymers (SIS), containing spherical, cylindrical, and lamellae structures, were prepared by solvent casting methods. The electrorheological properties of the films were investigated under oscillatory shear mode at electric field strengths of 0, 1 and 2 kV/mm as functions of temperature. In two SIS systems, the storage moduli ( $G'$ ) linearly increase with temperature up to 330 K at 1 rad/s in absence of electric field. The storage modulus responses increased with increasing of electric field upto 1 and decrease beyond that. In deflection experiments, under applied electric field, the deflection distances of D1114P and D1164P show stepwise increases with increasing electric field strength along with their dielectrophoretic forces, while another SIS system shows zero response towards applied electric field.

**Keywords:** Electrorheological properties; Styrene-Isoprene-Styrene; triblock copolymer, morphology; Dynamic moduli

\* Corresponding author.

*Email address:* [anuvat.s@chula.ac.th](mailto:anuvat.s@chula.ac.th), Tel: 662 218 4131, Fax: 662 611 7221

## 1. Introduction

Electro-active polymers (EAP) have received much attention in developing devices in actuation applications such as insect-like actuators and artificial muscles (Krause *et al.*, 2001) [1]. These materials have the intrinsic ability to convert electrical energy into mechanical energy. There are several candidate materials for those applications: conductive polymers, ferroelectric polymers, electro-active polymers, and dielectric elastomers (Zhang *et al.*, 1998, Pelrine *et al.*, 1998, and Kim *et al.*, 2007) [2-4]. Elastomer, a dielectric material, is a type of electric-field-activated electro-active polymers, which is capable of producing fast response, large strains, and relatively high efficiency (Kornbluh *et al.*, 2002) [5].

Various dielectric elastomers have been studied for the actuation: such as polyisoprene (Puvaratvttana *et al.*, 2008) [6], nitrile rubber (NBR) (Cho *et al.*, 2006) [7], and EDPM (Faez *et al.*, 2002) [8]. Styrene-isoprene-styrene triblock copolymer (SIS) is a thermoplastic elastomer which has similar useful properties to those of polyisoprene: flexibility, high tensile strength, and low swelling in water. These characteristics are required for actuation response under applied electric field. Triblock copolymers are widely known as composite materials having soft and rubbery matrix of isoprene in intimate contact with a hard and glassy domain of styrene. The reinforcing of styrene segment can increase the modulus and the yield strength relative to polyisoprene alone. Moreover, it is also acting as physical crosslink resulting in a copolymer exhibiting elastomeric properties of a crosslinked rubber that can easily be processed by conventional means (Lee *et al.*, 2006) [9].

For many years, SIS block copolymer morphology has attracted attention of many researchers because it has many valuable mechanical properties. The microphase separation structure is due to the incompatibility between the connected different block chains. SIS morphology can be divided into three different morphological types, such as lamellae, cylindrical, and micellar depending on styrene content. They are obtained from various techniques such melting, shearing, from different casting solvents (Wang *et al.*, 2001) [10], and solvent casting of different copolymer compositions (Winter *et al.*, 1993) [11]. The last one is the widely used technique to prepare these morphologies.

In this work, we are interested in the effect of SIS copolymer morphology on the mechanical properties, viscoelastic properties, and electrical properties with regard to actuation applications under electric field. These properties are investigated in terms of morphology (spherical, cylindrical, and lamellae), operating temperature, and electric field strength.

## 2. Experimental

### 2.1 Materials

SIS triblock copolymers, Kraton D1162P 44%styrene, Kraton D1164P 29%styrene, and Kraton D1114P 19%styrene (Kraton Polymers U.S. LLC) were used as the dielectric elastomers. Toluene (Lab Scan, AR grade) was used as the solvent.

### 2.2 Preparations of SIS films

SIS triblock copolymers, D1114P, D1164P, and D1162P were used to prepare films with three different morphologies: lamellae, cylindrical, and micellar; respectively. By Winter *et al.* (1993) [11] method, the films were cast from 10 % (w/v) toluene solution at room temperature for a duration of 1 week. To further remove toluene and reduce stresses from the solvent evaporation, the films were vacuum-dried at 120 °C for 24 h.

### 2.3 Characterization and testing of SIS films

Morphologies of SIS films (D1114P, D1164P, and D1162P) were observed by a polarizing optical microscope (Leica/DMRXP). The films were firstly freeze dried in liquid nitrogen and placed into microscope slides. Optical micrographs of the films were obtained with magnifications of 200 and 500 times.

Scanning electron micrographs were taken with a scanning electron microscope (JEOL, model JSM-5200) to determine the morphology of SIS films; D1114P, D1164P, and D1162P. The scanning electron micrographs of the films were obtained by using an acceleration voltage of 15 kV with magnifications of 1500 and 2000 times.

A Transmission electron microscope (Hitachi H-800) was used to observe SIS films morphologies. The sample films are embedded in an epoxy resin and cured

at 80 °C for 12 h. Ultrathin sections were cut from the embedded specimens by using an ultramicrotome, Reica Ultracut FCS, and a diamond knife in liquid nitrogen. To enhance a contrast, the ultrathin sections of the sample films are stained with osmium tetroxide and operated under the acceleration voltage of 100 kV.

Electrical conductivity of SIS films were measured by using a resistivity test fixture (Keithley 8009 resistivity test fixture) connected with a source power supplier (Keithley/ Model 6517A). The measurement was performed under atmospheric pressure, 40-60 %RH and at 25-27°C. The regime where responsive current is linearly proportional to the applied voltage is called the linear Ohmic regime. The voltage and the current in the regime were converted to the electrical conductivity by following equation:

$$\sigma = \frac{1}{\rho} = \frac{t \times I}{22.9 \times V} \quad (1)$$

where  $\sigma$  is specific conductivity (S/cm),  $\rho$  is the specific resistivity ( $\Omega \cdot \text{cm}$ ),  $t$  is the sheet resistivity ( $\Omega$ ),  $I$  is the measured current (A),  $V$  is the applied voltage (voltage drop) (V).

The electrorheological properties were investigated by using a melt rheometer (Rheometric Scientific, ARES). It was fitted with a custom-built copper parallel plates fixture (diameter of 25 mm). A DC voltage was applied with a DC power supply (Instek, GFG 8216A), which can deliver electric field strength to 2 kV/mm. A digital multimeter was used to monitor the voltage input. The oscillatory shear strain was applied and the dynamic moduli ( $G'$  and  $G''$ ) were measured as functions of frequency, temperature, and electric field strength. Strain sweep tests were first carried out to determine the suitable strains to measure  $G'$  and  $G''$  in the linear viscoelastic regime. The appropriate strains of SISs films; D1114P, D1164P, and D1162P are 0.2, 0.1, and 0.2 %, respectively. The frequency sweep tests were carried out to measure  $G'$  of each sample as functions of frequency, temperature, and electric fields (0, 1, and 2 kV/mm). The deformation frequency was varied from 0.1 to 100 rad/s. Each sample was presheared at a low frequency (0.039811 rad/s), and then the electric field was applied for 30 minutes to ensure the formation of equilibrium polarization before the  $G'$  measurements. Experiments were carried out at the temperature of 27 °C and repeated at least two or three times. The effect of

temperature in SISs films was studied at various temperatures in the range of 27-117 °C. For the effect of electric field strength the experiments were taken at various electric fields (0, 1, and 2 kV/mm). Temporal response measurements of pure SIS films were carried out at electric field strength 0 and 2 kV/mm.

Deflection of SIS films were carried out under various applied electric strengths. For each of films, one end of the sample was fixed with grip vertically in the chamber, which consisted of two electrodes and poly(dimethylsiloxane). The input DC field was generated by a DC power supply (Gold Sun 3000, GPS 3003D) and a high voltage power supply (Gamma High Voltage, UC5-30P) which delivered to the electrodes various electric fields from 25 to 600 V/mm. A video recorder was used to record the displacement of the film made a model. The tip displacement was measured through a Scion Image (Beta 4.0.3) program

### 3. Results and Discussion

#### 3.1 Characterization of SIS films

The SEM micrographs of SIS films are shown in Figure 1. The surface morphology of SIS films shows that D1162 have smoother surface than that of D1164P and D1114P, due to polystyrene content of each sample.

The specific conductivity of SIS films; D1114P, D1164P, and D1162P were investigated by using a resistivity test fixture (Keithley 8009 resistivity test fixture) worked with a source power supplier (Keithley/ Model 6517A). The specific conductivity of D1114P, D1164, and D1162P are  $1.28 \times 10^{-19}$ ,  $2.69 \times 10^{-17}$ , and  $1.17 \times 10^{-17}$  S/cm with standard deviations of  $1.58 \times 10^{-20}$ ,  $0.32 \times 10^{-18}$ , and  $1.00 \times 10^{-18}$  S/cm, respectively.

#### 3.2 Electrorheological Properties of SIS

The rheological properties of the SIS films were investigated at electric field strengths of 0, 1 and 2 kV/mm with the temperature range of 300 to 390 K, and vary frequency 0.1 to 100 rad/s. Here we used one sample each for the  $G'_o$ ,  $G'_{1kV/mm}$ , and  $G'_{2kV/mm}$  measurements. Figure 2(a) shows the frequency sweep performed by using strain of 0.2 % at various temperature of D1114P which is consisting of

spherical microphase structure. The responses can be divided in three regimes. At below 330 K (57°C), the storage moduli ( $G'$ ) without applied electric field appears to be plateau independent of frequency ( $\omega = 0.1-100$  rad/s). The D1114P system exhibits an elastic rubbery-like response. In the temperature range of 330-360 K (57-87°C), the detected moduli ( $G'$ ) appear to slightly increase with frequency in non-linear fashion up to  $\omega = 100$  rad/s. The character here is of the plastic response (Sato *et al.*, 1996). This plastic behavior is related to microdomain structure of polystyrene segment which is still preserved at these immediate temperatures which are in a softened state. At high temperature above 360 K (87°C), the moduli at low frequency decrease abruptly with increasing of temperature; at each temperature the moduli appear to dramatically increase non-linearly with frequency. This behavior is of the viscous transition regime (Sato *et al.*, 1996). These behaviors are also found in the frequency sweep tests of D1164P and D1162 films having cylindrical and lamellae morphologies at ambient temperature. Sato *et al* (1996) [12] reported the similar responses of SIS copolymers.

The increases in the storage modulus with increasing temperature without applied electric field of the SIS copolymers (D1114P, D1164P, and D1162P) are shown in Figures 2(b)-(d), at the frequency of 1 rad/s. The change in the storage moduli ( $G'_o$ ) of each system can be referred to the rubbery-plastic-viscous transitions. In the figures, the storage moduli ( $G'_o$ ) are compared to those at various applied electric field strengths, 1 and 2 kV/mm. Electric field was first applied on each sample for a period of 30 minutes before  $G'_{1kV/mm}$  and  $G'_{2kV/mm}$  were measured successively at each temperature. From Figures 2(b)-(d), it can be seen that  $G'_o$ ,  $G'_{1kV/mm}$ , and  $G'_{2kV/mm}$  linearly increase with temperature above 330 K (57°C) then decrease after 360 K (87°C), identifying the plastic regime and the viscous regime, respectively. In addition,  $G'_{1kV/mm} > G'_{2kV/mm} > G'_o$  at all temperatures in the plastic regime. It may be noted that the changes in the storage moduli with temperature have been shown to be accompanied with the changes in dielectric constant (Sato *et al.*, 1996) [12].

Because of an applied electric field, electrical dipole moments are generated and the electrostatic interaction between the polymer chains occurs leading to an intermolecular interaction acting like an electrical network. The electrostatic

interaction causes a compressive force on the dielectric elastomer or SIS films in the direction of electric field. This effect can be described in term of actuation pressure by (Pelrine *et al.*, 2000) [13]:

$$p = \varepsilon\varepsilon_0 E^2 \quad (2)$$

where  $E$  is the electric field,  $\varepsilon$  is the dielectric constant,  $\varepsilon_0$  is the permittivity of free space. As in equation (1), when electric field is applied to SIS films, a greater pressure is generated in the SIS film and  $G'$  exhibits a higher value than that without electric field. Also, the increasing of  $G'$  with electric field strength in plastic regime of D1114P, D1164P, and D1162P are consistent with the classical network theory in equation (2) (Rubinstein *et al.*, 2003) [14]:

$$G' = \nu_e k_B T \quad (3)$$

where  $k_B$  is Boltzmann's constant,  $T$  is the absolute temperature (K), and  $\nu$  is number of electrical strands per unit volume ( $\text{cm}^{-3}$ ). Since the elastomers are unmodified and no crosslinks exist, the linear dependence of  $G'_0$ ,  $G'_{1\text{kV/mm}}$  and  $G'_{2\text{kV/mm}}$  on  $T$  presumably stems from physical entanglements. From the responses of storage moduli ( $G'$ ) at 1 kV/mm of D1114P, D1164P and D1162P; they are than the others, presumably due the dipole-dipole interactions within the matrix and the increases in the dielectric constant in the plastic regimes. The slopes of the moduli vs. temperature at 1 kV/mm are steeper than others. From equation (2), we can calculate  $\nu_e$  from slope of the linear responses of D1114P and D1164P from Figures 2(b)-(c).  $\nu_e$  data are shown in Table 1 for each sample, the number of electrical strand per unit volume at 1 kV/mm is higher than that at 0 and 2 kV/mm in both morphology systems. The similar effect of electric field was also reported by Kunanuruksapong *et al.* (2007) [15], the effect of tempeature on the rheological properties of prestine elastomer (AR71) was carried out at 0 and 2 kV/mm. They found that the  $\nu_e$  at 2 kV/mm is higher than  $\nu_e$  in the absence of electric field.

However, in temporal response measurements, the pure SIS films does not exhibit response whereas at 300 K or at temperature of 360 K under an alternately applied electric field.

### 3.3 Deflection measurement of SIS films

In the deflection measurement, D1114P, D1164P, and D1162P bendings were observed and measured in response to electric field. The samples were gripped between copper plates and immersed in the poly (dimethylsiloxane). The positive current was applied to the copper plate as shown in Figure 3. A video recorder was used to record the tip displacement of the film as shown in the model. The deflection distance in x axis ( $d$ ) and deflection length ( $l$ ) were measured through the analysis program. The deflection angle was determined by calculating of arc tan between  $d$  and  $l$ .

As the electric field is applied, the free end of the SIS films bend towards the anode site because the attractive interaction between electric field induced dipole moment in SIS matrix and the anode. In Figure 4, circular and triangular symbols represent the tip displacement distances of D1114P (spherical) and D1164P (cylindrical) which were observed and the square symbol represents D1162P (44 %wt PS) displacement data which appear not to response under applied electric field. In cases of D1114P and D1164, the films deflections exhibit stepwise bending responses with increasing electric field strength. The D1114P film show greater deflection values than those of others. Moreover, the film starts its deflection at a lower applied electric field strength, 150 V/mm, and at 250 V/mm for D1114P and D1164P, respectively. These deflections here are due to the electric field induced dipole-dipole interactions. Nevertheless, the reinforcing phase structure of polystyrene within the soft and flexible phase may also influence the deflection of the films through the increase in the storage moduli ( $G'$ ) of the copolymer. For the lamellae microphase D1162P system reinforcing the isoprene phase, the film is hardly deflected by the electric field induced dipole-dipole interactions. In the case of D1164P, the rod-like hard phase of styrene induces the D1164P modulus to be higher than that of D1114P which has a spherical styrene microdomain, therefore D1114P is more responsive than D1164P.

Form force balance, the deflection force or dielectrophoretic force ( $F_d$ ) of the samples is equal to the incorporation of elastic force ( $F_e$ ) and the weight along the bending direction, where the film deflection distance at equilibrium is  $d$ . The dielectrophoretic force (N) is calculated from the following equation:



$$F_d = F_e + mg \sin \theta \quad (4)$$

where  $m$  is the sample's weight (kg),  $g$  is the gravity ( $9.8 \text{ m/s}^2$ ),  $\theta$  is the deflection angle, and  $F_e$  is the resisting elastic force (N). In our experiment, the film deflections with increasing of electric field are non-linear. Therefore, we used the non-linear deflection theory of one free-end film where the elastic force can be calculated as in the following equation (4) (Timoshenko *et al.*, 1970 and Gere *et al.*, 1972) [16,17]:

$$F_e = \frac{dEI}{l^3} \quad (5)$$

where  $E$  is modulus of elasticity equal to  $2G'(1+\nu)$ ,  $G'$  is the shear modulus,  $\nu$  is Poisson's ratio which is equal to  $1/2$  for an incompressible material,  $I$  is the moment of inertia equal to  $t^3w/12$  which  $t$  is the sample thickness,  $w$  is the sample width,  $d$  is the deflection distance ( $d$ ), and  $l$  is the sample length.

From Figure 5, the dielectrophoretic force of the pure D1114P and D1164P systems appear to increase stepwise with increasing of electric field except D1162P. Moreover, force density and energy density also show similar behaviors with increasing electric field as tabulated in Table 2. However, these are apparent forces calculated from Equations (4) and (5) but may not represent the true force is represented by the filled symbols. Apparent force is represented by the unfilled symbols which are always less or equal to the true force.

Niamlang *et al.* [18] reported a dependence of applied voltage on the dielectrophoresis force of polydimethylsiloxane (PDMS) under the effect of cross-linking ratio. The PDMS films were suspended in silicone oil under applied electric field between two parallel plates. They found that the force increased linearly with the electric field strength and  $F_d$  was higher when the cross-linking ratio was varied from 0.001 to 0.01. Because the lower cross-linking system has a lower number of strands in the PDMS network, it therefore has a lower capability to produce the force. Our SIS system with PS content of 44 %wt (D1162P) shows a lower  $F_d$  than those D1114P and D1164P. This is because the high PS content system possesses a higher number of strands, however the hard phase PS strongly obstructs the bending due to the induced force.

#### 4. Conclusion

In our work, electrorheological properties of styrene-isoprene-styrene triblock copolymers were investigated by examining the effect of morphology on the dynamic storage modulus ( $G'$ ), under oscillatory shear mode. The experiments were carried out with electric field strengths of 0, 1 and 2 kV/mm, with temperature and frequency sweep mode. In our SIS material systems consisting of spherical (D1114P), cylindrical (D1164P), and lamellae (D1162P) systems, their storage modulus exhibit linear increases with increasing temperature beyond 330 K at 1 rad/s. Moreover, the responses are higher at the electric field 1 kV/mm. The increases in the storage modulus response can be traced back to the rising temperature which tends to increase the dielectric constant, and the effect of applied electric field which induces the electrical network within the SIS matrix.

From the deflection measurement, the deflection distances of D1114P and D1164P increase stepwise with increasing of electric field along with corresponding dielectrophoretic forces, while D1162P shows no deflection response. When electric field induced force is not high enough to overcome the resisting elastic force the film shows no response. This is apparently the case of D1162P system which has the hard lamellae morphology, whereas the spherical morphology of D1114P shows the greater response than the others.

#### 5. Acknowledgement

The authors would like to acknowledge the financial supports to A.S from the Conductive and Electroactive Polymers Research Unit of Chulalongkorn University, the Thailand Research Fund (BRG), the Petroleum and Petrochemical and Advanced Materials Consortium, the Thai Royal Government (Budget of Fiscal Year 2551), the Shell (Thailand) Company Limited and Toyota Tsusho (Thailand) Company Limited for the materials: Kraton D series.

## 6. References

- [1] S. Krause K. Bohon, *Macromolecules* 34 (2001) 7179-7189.
- [2] Q.M. Zhang, V. Bharti, X. Zhao, *Science* 280 (1998) 2101–2104.
- [3] R.E. Pelrine, R.D. Kornbluh, J.P. Joseph, *Sensor Actuat. A* 64 (1998) 77-85.
- [4] J. Kim, Y. Kangand, S. Yun, *Sensor Actuat. A* 133 (2007) 401-406.
- [5] R. Kornbluh, R. Perlrine, Q. Pei, S. Oh, J. Joseph, *Pro. of The first World Congress on Biomimetics* (2002).
- [6] T. Puvanattvattana, D. Chotpattananont, P. Hiamtup, S. Niamlang, R. Kunanuruksapong, A. Sirivat, A.M. Jamieson, *Mat. Sci. Eng. C* 28 (2008) 119–128.
- [7] M.S. Choa, H.J. Seo, J.D. Nam, H.R Choi, J.C. Koo, K.G. Song, Y. Lee, *Sensor Actuat. B* 119 (2006) 621–624.
- [8] R. Faez, R.H. Schuster, M.A. De Paoli, *Eur. Polym. J.* 38 (2002) 2459–2463.
- [9] W.K. Lee, H.D. Kim, E.Y. Kim, *Curr. Appl. Phys.* 6 (2006) 718-722.
- [10] Y. Wang, J.S. Shen, C.F. Long, *Polymer* 42 (2001) 8443-8446.
- [11] H.H. Winter, D.B. Scott, W. Gronski, S. Okamoto, T. Hashimoto, *Macromolecules* 26 (1993) 7236-7244.
- [12] T. Sato, H. Watanabe, K. Osaki, *Macromolecules* 29 (1996) 6231-6239.
- [13] R. Pelrine, R. Kornbluh, J. Joseph, R. Heydt, Q. Pei, and S. Chiba, *Mat. Sci. Eng. C* 11 (2000) 89-100.
- [14] M. Rubinstein, R.H. Colby, *Polymer Physics* (2003) 298-300.
- [15] R. Kunanuruksapong and A. Sirivat, *Mat. Sci. Eng. A* 454–455 (2007) 453–460.
- [16] S.P Timoshenko, J.N. Goodier, *Theory of elasticity*, 3rd ed., McGraw-Hill, Auckland, 1970, pp. 41-46.
- [17] J.M. Gere, *Mechanics of Materials*, 3<sup>rd</sup> ed., Chapman & Hall, 1972, pp. 515-516.
- [18] S. Niamlang and A. Sirivat, *Macromol. Symp.* 264 (2008) 176-183.

**Table 1** Number of electrical strands ( $v_e$ ) per unit volume of D1114P, D1164P, and D1162P at various electric field strengths versus temperature

Sample	Applied electric field (kV/mm)	Strain (%)	$v_e$ (cm <sup>-3</sup> ) at $\omega = 1$ rad/s	$v_e$ (cm <sup>-3</sup> ) at $\omega = 100$ rad/s
D1114P	0	0.2	$2.10 \times 10^{21}$	$5.58 \times 10^{21}$
	1	0.2	$2.89 \times 10^{21}$	$7.05 \times 10^{21}$
	2	0.2	$1.89 \times 10^{21}$	$4.15 \times 10^{21}$
D1164P	0	0.1	$1.82 \times 10^{21}$	$3.94 \times 10^{21}$
	1	0.1	$2.91 \times 10^{21}$	$6.54 \times 10^{21}$
	2	0.1	$2.05 \times 10^{21}$	$5.32 \times 10^{21}$
D1162P	0	0.2	N/A	N/A
	1	0.2	N/A	N/A
	2	0.2	N/A	N/A

**Table 2** Electromechanical responses of pure SIS, D1114P, D1164P, and D1162P at various electric field strengths

Sample	E (V/mm)	d (mm)	l (mm)	$\theta$ (°)	mg sin( $\theta$ ) ( $\mu$ N)	$F_e$ ( $\mu$ N)	$F_d$ ( $\mu$ N)	$\tau_i$ (sec)	$\tau_r$ (sec)	Energy density (J/m <sup>3</sup> )	Force density (N/m <sup>3</sup> )
D1114P	0		15.31								
	100		15.31								
	200	0.61	15.31	2.3	7.14	0.549	7.69	30	4	80.8	387.5
	300	0.61	15.31	2.3	7.14	0.549	7.69	40	8	80.8	387.5
	350	1.02	15.31	3.8	11.9	0.918	12.8	44	9	225.6	647.6
	400	1.02	15.31	3.8	11.9	0.918	12.9	49	14	225.6	647.6
	450	1.43	15.31	5.4	16.7	1.29	18.0	50	15	442.8	907.6
	500	1.63	15.31	6.1	19.1	1.48	20.5	54	17	574.8	1034.2
	550	2.65	15.31	9.9	30.9	2.45	33.3	54	28	1509.9	1679.0
	600	2.86	15.1	10.9	33.8	2.65	36.4	55	33	1804.4	1834.2
	D1164P	0		14.68							
100			14.68								
200			14.68								
300		0.21	14.68	0.8	2.52	0.393	2.92	29	6	16.5	155
350		0.21	14.68	0.8	2.52	0.394	2.92	30	7	16.5	155
400		0.43	14.68	1.7	5.16	0.806	5.97	33	10	69.3	318
450		0.64	14.68	2.5	7.68	1.20	8.89	39	10	153.4	473
500		0.64	14.68	2.5	7.68	1.20	8.89	43	13	153.4	473
550		0.64	14.68	2.5	7.68	1.20	8.89	45	13	153.4	473
600		1.07	14.68	4.2	12.8	2.00	14.9	49	16	428.3	791
D1162P	0		15.53								
	200		15.53								
	400		15.53								
	600		15.53								

\*\*  $d$  = deflection distance along the horizontal axis (mm)

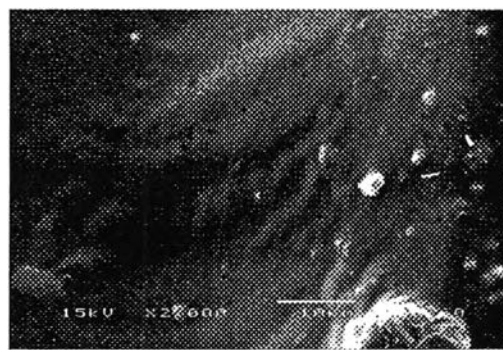
$l$  = deflection distance along the vertical axis (mm)

$F_e$  = elastic force (N) =  $\frac{dEI}{l^3}$  for non linear deflection

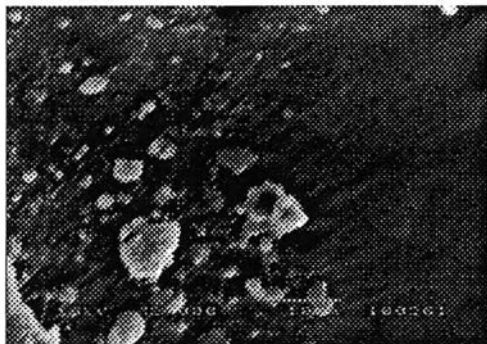
$F_d$  = dielectrophoretic force =  $F_e$  (N) +  $mg \sin\theta$

$\tau_i$  = induction time (sec)

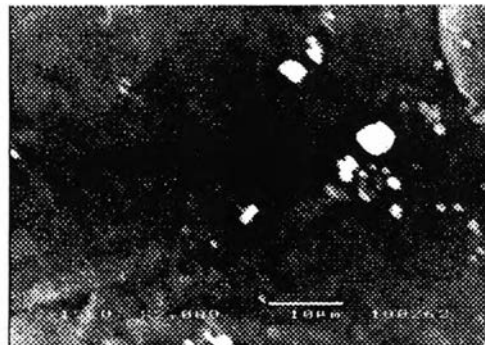
$\tau_r$  = recovery time (sec)



(a)

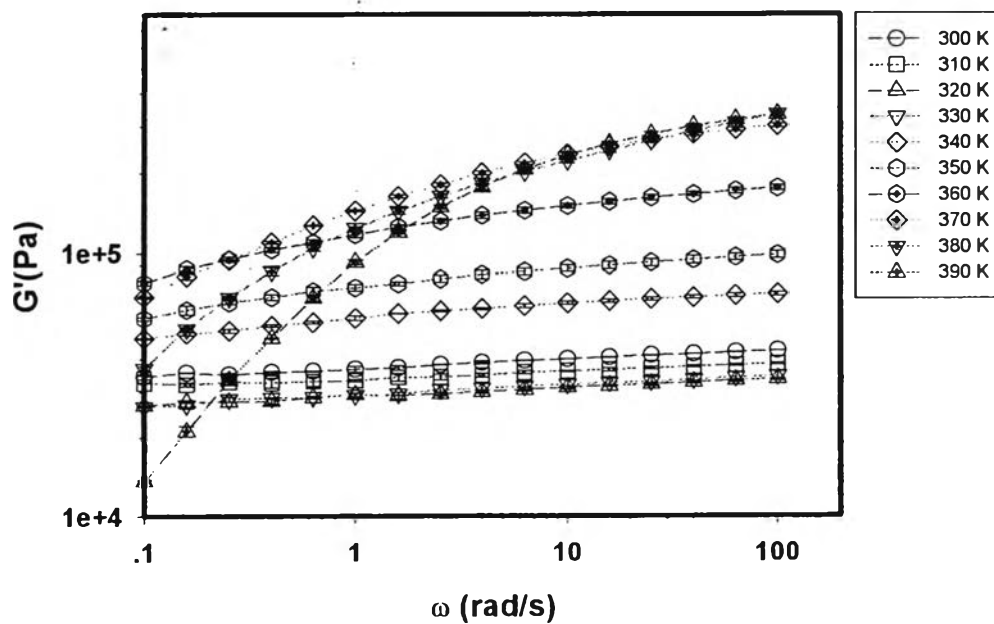


(b)

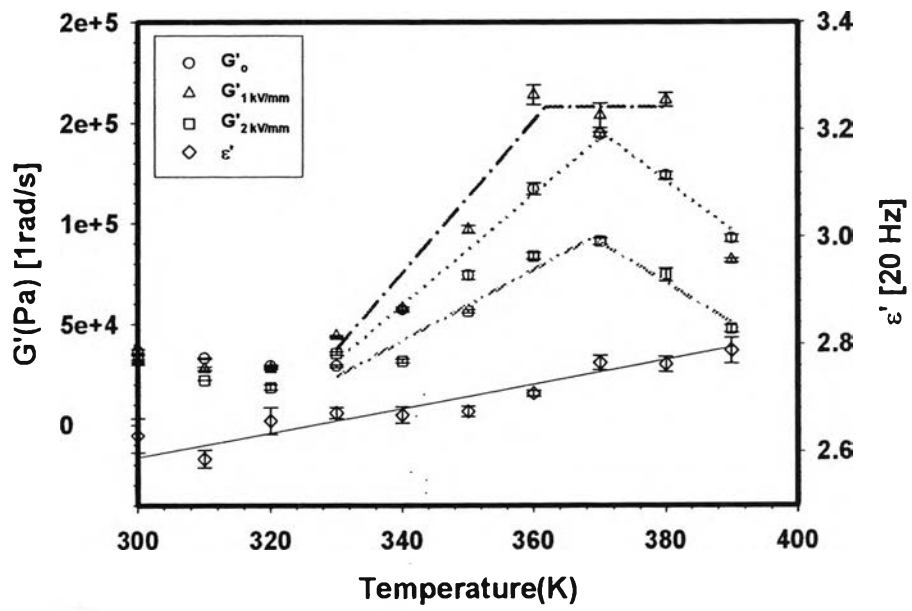


(c)

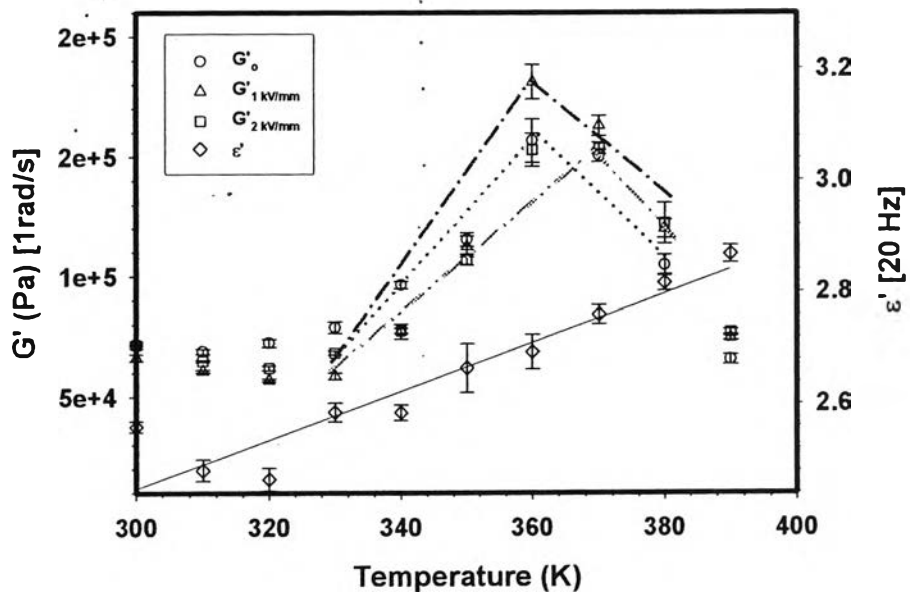
**Figure 1.** SEM micrographs: (a) SIS D1114P (19 wt% PS) film at magnification of 2000, 15 kV; (b) SIS D1164P film at magnification of 2000, 15 kV; and (c) SIS D1162P film at magnification of 2000, 15 kV.



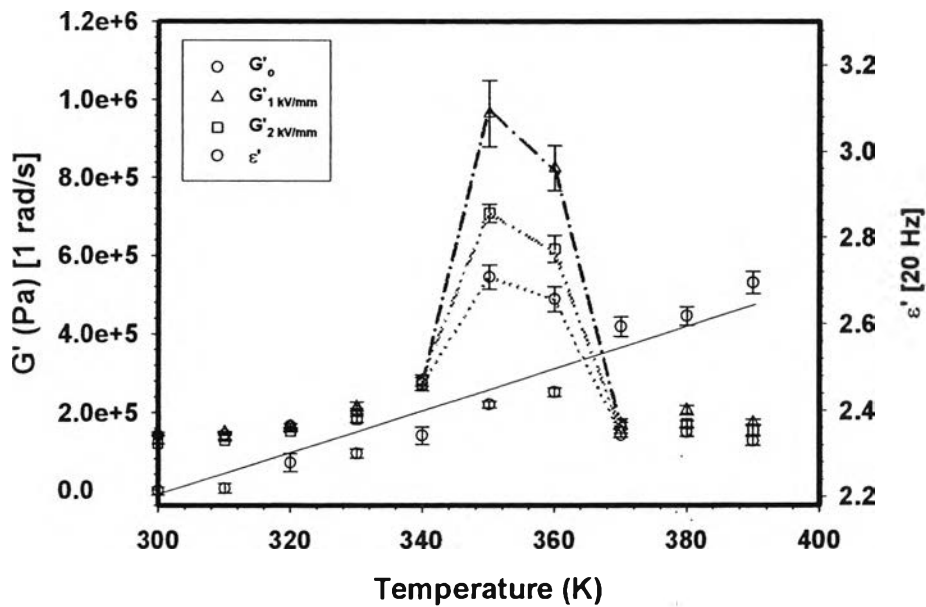
(a)



(b)



(c)



(d)

**Figure 2** Comparison of storage modulus exhibited at different temperatures under various electric fields: (a) frequency sweep test of D1114P at  $E = 0$  V/mm under various temperatures; (b)  $G'$  of D1114P and dielectric constant vs. temperature at frequency 1 rad/s, strain 0.2 %; (c)  $G'$  of D1164P and dielectric constant vs. temperature at frequency 1 rad/s, strain 0.1 %; and (d)  $G'$  of D1162P and dielectric constant vs. temperature at frequency 1 rad/s, strain 0.2 %.

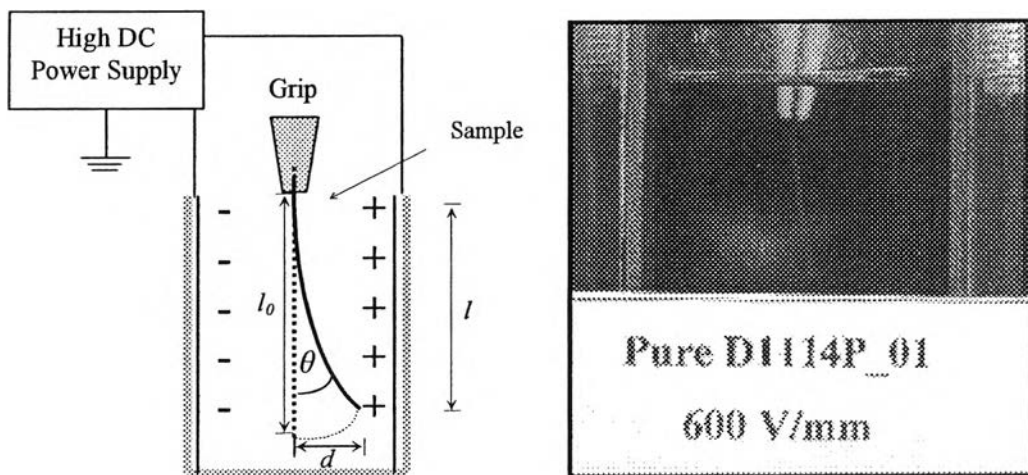


**Figure 3** Deflection of the sample under electric field.



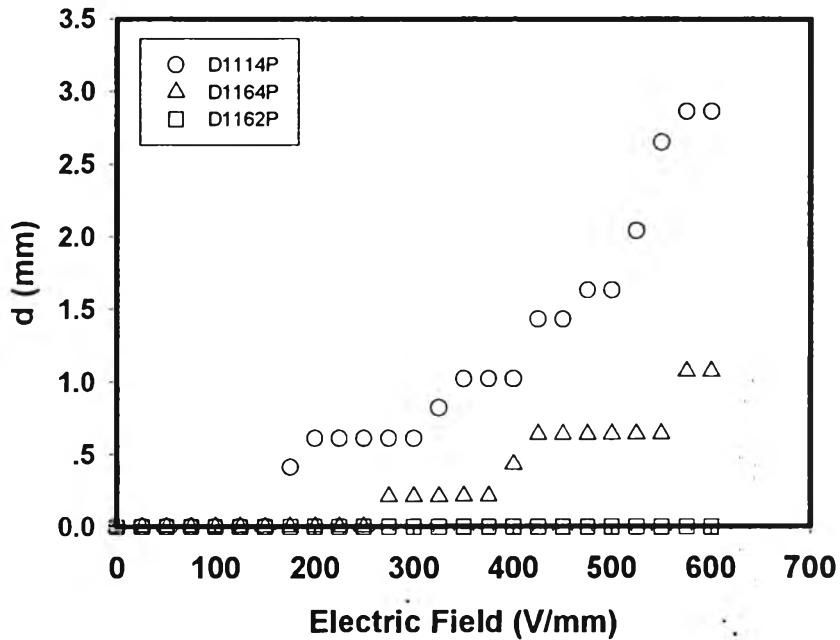


**Figure 4** Deflection distances of pure SIS, D1114P, D1164, and D1162P at various electric field strengths calculated through the Non-Linear Deflection theory.

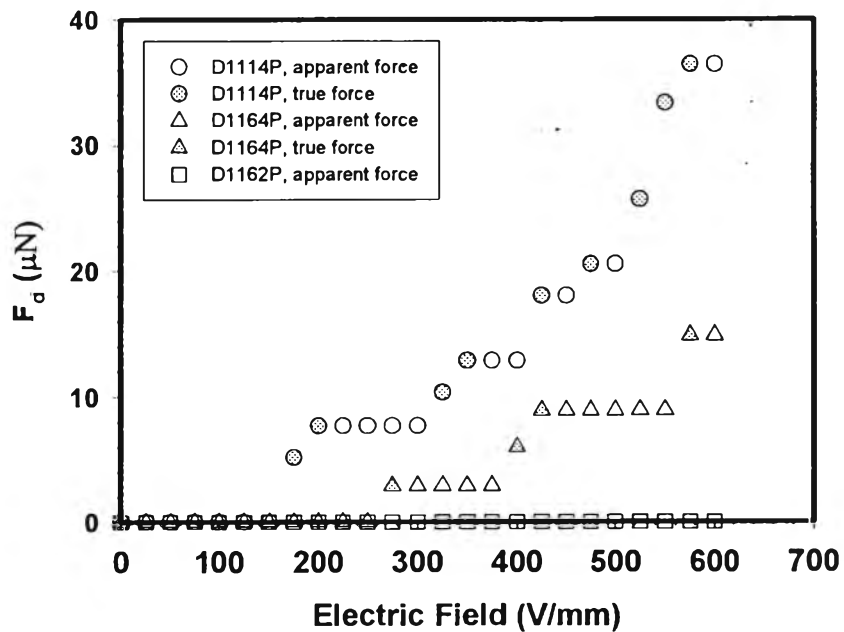


**Figure 5** Dielectrophoretic forces of pure SIS, D1114P, D1164, and D1162P at various electric field strengths calculated through the Non-Linear Deflection theory.